Available online at www.sciencedirect.com

jmr&t Journal of Materials Research and Technology

journal homepage: www.elsevier.com/locate/jmrt

Original Article

Optimized epoxy foam interface of CFRP/Epoxy Foam/CFRP sandwich composites for improving compressive and impact properties

Dong-Jun Kwon [a], *Jong-Hyun Kim* [a,b], *K. Lawrence DeVries* [c], *Joung-Man Park* [a,b,c,*]

[a] *Research Institute for Green Energy Convergence Technology, Gyeongsang National University, Jinju, Republic of Korea*

[b] *Department of Materials Engineering and Convergence Technology, Gyeongsang National University, Jinju, 52828, Republic of Korea*

[c] *Department of Mechanical Engineering, The University of Utah, Salt Lake City, Utah, 84112, USA*

ARTICLE INFO

Article history:
Received 9 November 2020
Accepted 5 January 2021
Available online 9 January 2021

Keywords:
Fabrication process
Epoxy foam (EF)
Sandwich composite
Micro-mechanics

ABSTRACT

Composite materials for vehicle parts require lightweight, high strength and good impact properties. In this study, the optimized manufacturing conditions of epoxy foam (EF) were investigated to improving mechanical performance of carbon fiber reinforced plastic (CFRP)/EF/CFRP sandwich composites for vehicle parts such as impact, flexural property. The optimal curing temperature was found to be 60 °C, by measuring the reaction rate, volume increase rate, density, cell size, glass transition temperature, and specific compressive strength of the EF. In addition, foams after 180 °C thermal aging were observed, and the properties of the EF cured at 60 °C were the most stable under the thermal aging. The performance of the sandwich EF composites was investigated using compressive, flexural strength, lap shear strength, and impact tests. The optimized cell condition of the EF was correlated to improving interfacial adhesion of sandwich composite.

1. Introduction

Diverse research and test methods had been developed and used to increase the use of composite materials for vehicle parts, but the increased use of high strength metals and economic issues of CFRP still limits their use [1]. Sandwich type composite materials with improved economic efficiency by reducing the thickness of CFRP have been developed to better utilize composite parts taking advantage of their functionalities such as light weight and impact properties in transportation, aerospace and marine fields [2,3]. Generally, honeycomb structures have been used to manufacture sandwich type composites [4], but Al foam and other core types

* Corresponding author.
E-mail address: jmpark@gnu.ac.kr (J.-M. Park).

https://doi.org/10.1016/j.jmrt.2021.01.015

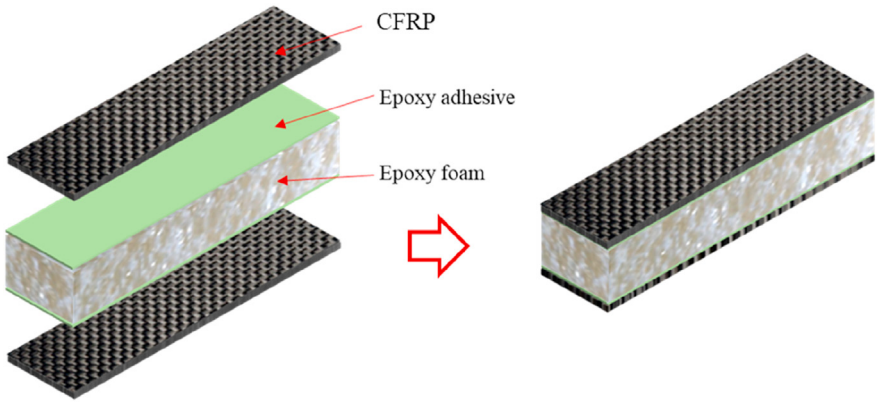

Fig. 1 – Schematic of the specimen manufacturing process.

have also been widely used [5]. The Airbus A340, for example, has its entire vertical tail made of composite sandwich structures, composed of glass fiber reinforced prepreg with a Nomex® honeycomb core [6]. Aluminum foam exhibits an excellent combination of physical and mechanical properties to resist impact and blast loading [7]. In the case of polymer foam materials, the use of sandwich composites using polyethylene terephthalate (PET) foam or polyvinylchloride (PVC) foam (3A Co.), have been used in Mercedes-Benz A series automobiles [8,9].

Impact absorption and interfacial stability between skin layer and core layer are critical issues in the manufacture of sandwich composites [10]. A simple fabric surface brushing and abrading method to improve interfacial adhesion between CFRP and core materials has been developed and demonstrated to significantly enhance the delamination resistance of sandwich composites with only moderate in-plane tensile strength loss [11]. In one research project, the magnetorheological elastomer (MRE) tapered composite sandwich plate configuration was found to secure the interfacial structure of a sandwich composite [12]. Attempts had been made to enhance the properties of sandwich composites using nanoparticles to improve foam mechanical properties and to enhance impact absorption by varying specimen thickness [13]. In addition, the properties of sandwich composite materials using modified polymer structural foams of varying foam compositions have been studied [14,15].

Structural stability of sandwich composites can be improved by improving the adhesion between the skin layer and the core material, and by utilizing the optimal design technology suited to the conditions of use [16,17]. A stable core cell structures has been developed through the improvement of the inner core structure and analysis using Abaqus [18]. In particular, structural foam can be easily modified by varying the types of raw material. A motivation for several material studies, is the fact that sandwich composite materials can be effectively used not only for vibration [19] and noise canceling applications [20], but They also have other functionalities such as electromagnetic shielding [21].

In general, core type reinforcement has been used more than the foam type reinforcement in the manufacture of sandwich composites to improve the composite's mechanical strength [22]. However, foam type reinforcement, with a specific gravity lower than that of core reinforcement, has advantages in terms of specific tensile strength and specific compressive strength of sandwich composites [23]. Furthermore, foam type reinforcement, which is typically manufactured using more eco-friendly raw materials, may result in more eco-friendly composite usage. Foam materials might also be used to increase the electrical conductivity [24] and other multi-fuctional properties in sandwich composites by adding dispersed nanoparticles in the "novel" foam [25,26].

Generally, polyurethane (PU) foam is the most widely used material for these composites. However, PU foam is more unstable in strength, durability and heat resistance than epoxy foam. From Kwon's previous works [27,28], PET, PVC, and PU foams, which were known as structural foams, had unstable heat resistance compared to epoxy foam. In addition, it was confirmed that the epoxy foam was stable without deformation of shape or strength at 180 °C for 30 min coating process during vehicle manufacturing processes. Unlike polylactic acid (PLA) or polylactide, PU and polyvinylchloride (PVC) foams, research on sandwich composites using structural epoxy foams were best in areas requiring heat resistance and rigidity [29–31].

In this study, the optimum temperature for curing epoxy foam was investigated. The mechanical properties of sandwich composites were evaluated to verify the effect of the foam properties with different curing temperatures. The time at the 95% degree of cure was confirmed by differential scanning calorimetry (DSC). The effect of the curing temperature was analyzed using the apparent density and the cell size of epoxy foams. Thermal mechanical stability of the epoxy foams was evaluated by measuring T_g and specific compressive testing. The epoxy foam was aged at 180 °C and the fracture behavior was evaluated by the strength changes for epoxy foams with different aging times. Compression, flexural strength, adhesive strength and impact properties of the sandwich composites were correlated with each other. The advantages of sandwich composites using epoxy foams were demonstrated by comparing their impact properties with the impact properties of steel actually used in vehicles.

2. Experimental

2.1. Materials and fabrication of sandwich composites with structural epoxy foam

Fig. 1 shows the schematic processes used in the manufacture of the specimens. The epoxy foam (EF) specimens (2080M25, Resoltech, Inc., France) was used in combination with a curing agent (2085M, Resoltech, Inc., France) containing amine and isocyanate functional groups. The curing agent (2085M) was added to the epoxy (2080 M25) at a weight ratio of 3:7, and the mixture was stirred for 3 min at 500 rpm 150 ml of EF this solution was put into a 380 ml paper cup, and the epoxy foams were molded using different curing temperatures. The skin layer of the sandwich composite was fabricated using unidirectional CFs (UD CF) and woven CFs. The woven CF prepregs were positioned on the outsides and the UD CFs were laminated inside of the composite specimens at a [0/90] condition. Specimens were molded using a closed mold at 150 °C for 10 min. The UD CF prepreg and woven CF prepreg used which were fast curing type prepreg (TB Carbon co, Ltd, Korea). The CFRP plates were fabricated in a size of 300 mm × 300 mm x 2.4 mm under a pressurization of 1 MPa. These were then cut into a 20 mm × 80 mm x 2.4 mm size using a CMS waterjet. The plates were dried for 24 h at 60 °C and then bonded with the structural epoxy foams to fabricate the CFRP/EF sandwich composites.

2.2. Characterization of the epoxy foams with different curing temperatures

Foaming conditions and formation of the commercial EF material were investigated since the information was not readily available. Although curing at room temperature was recommended by the manufacturer, Resoltech, the formations of EF molded at different temperatures were analyzed because the curing time at room temperature takes too long. Characterization of the EF were conducted with curing temperatures of 25, 40, 60, 80, 100, 120, 140, 160, 180, and 200 °C. Curing time for with 95% degree of cure was measured by DSC (DSC 4000, PerkinElmer). The degree of cure of the EF was calculated using Eqn (1).

$$\alpha = \frac{\Delta H_t}{\Delta H_R} \tag{1}$$

where t was the curing time showing the cure state of 95% or more for the different temperature conditions, $\triangle H_t$ was the cumulative heating value until time t, and $\triangle H_R$ was ~~all~~ the heat of reaction generated for the raw materials.

The amount of foaming generated for the different curing temperatures was investigated, and the volume change rate of the generated foams was determined by comparing the increased volume with respect to the amount of the initial solution. The foams were then cut into a cubic size of 30 mm × 30 mm × 30 mm, and the apparent density of the EF was obtained using an analytical balance (XSE204V, Mettler Toledo Ltd, Korea) according to the ISO standard 845. The changes in the cell configuration of the EF were observed using an optical microscope (SMZ18, Nikon, Japan).

The glass transition temperature (T_g) of the cured epoxy foams was measured by DSC using 5.0 mg of the foams to analyze the change in thermal properties of the EF. The specific compressive strength of the EF as a function of the curing temperature was measured to ascertain optimal temperature conditions for enhancing mechanical and interfacial strength. The specific compressive strength was obtained by conducting compressive strength tests based on ISO standard 844. To determine the specific compressive strength these test results were divided by the density of the foam, measured with ISO standard 845. Finally, aging of the EF was carried out at 180 °C for 180 min to investigate thermal aging stability. Changes in the EF with the various curing temperatures and time of heating aging were observed, and changes in specific compressive strength were analyzed.

2.3. Mechanical characterization of sandwich composites

To fabricate the specimens, shown schematically in Fig. 1, CFRP plates and the EF, with different curing temperatures, were bonded with a D-type structural adhesive (Kospol Co., LTD., Korea). The average thickness of the adhesive was roughly 50 ± 10 μm. The sandwich composite specimens were cured at 180 °C for 10 min at a pressure of 1 MPa to bond the dissimilar materials. Compressive and flexural strength tests were performed according to ASTM standard C109 and ISO standard 178 on the specimens of reduced size. The specimens for compressive strength were made of cubes of 50 mm in height and length, and the flexural test specimens were fabricated of 20 mm in width, 40 mm in height and 80 mm in length.

To evaluate the adhesion between the CFRP plate and the EF, an adhesion test was performed using the evaluation methods of ASTM standard D5868, but with the shape of the specimens changed to a sandwich configuration. To prepare the sandwich type specimens, EF was cut into 20 mm × 20 mm × 10 mm size and inserted between 20 mm × 80 mm × 2.4 mm CFRP plates and bonded over a 20 mm × 20 mm area using the structural adhesive.

Impact properties of the CFRP/EF sandwich composites were obtained with an Izod impact tester (IT504, Tinius Olsen, U.S.A.). The pendulum of the impact tester can apply a maximum 25.3 J of energy to a specimen. The impact energy of a specimen during fracture was evaluated by striking a simply support beam of the material in the middle in the Charpy impact testing method. The specimens used for the impact test were fabricated with the same width of 20 mm and length of 80 mm but with differing thickness to compare the impact energies of specimens with different thicknesses. The impact properties of CFRP/EF sandwich composites (i.e., impact energy) and tensile strength of steels (Hyundai Steel, Korea) with different thicknesses were measured. The density of materials were 7.33 (SGAFC340), 7.65 (SGAFC590), 7.72 (SGAFC980), and 1.64 (CFRP), and average 0.56 g/cm^3 (CFRP/EF sandwich composite with different foam thickness). The density of CFRP/EP foam decreased from 0.73 to 0.34 g/m^3 as the EP foam thickness increased from 24.4 to 9 mm. Trend lines were evaluated by measuring the impact energy dependence on the thickness of CFRP, and the effect of thickness of the foams on

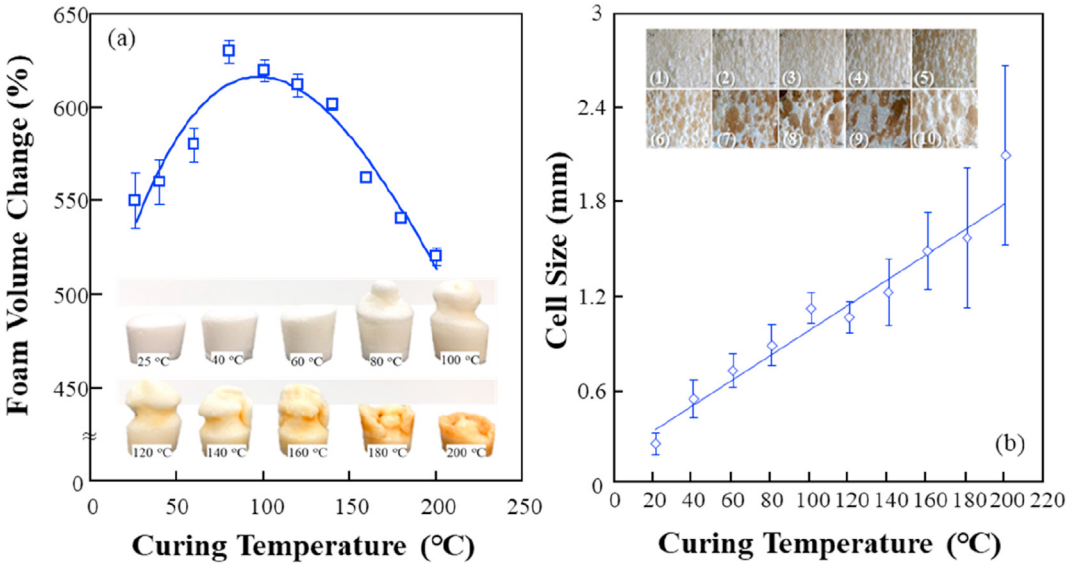

Fig. 2 – Some properties of epoxy foam cured at different temperatures: (a) volume change rate and (b) cell: (1) 25 °C; (2) 40 °C; (3) 60 °C; (4) 80 °C; (5) 100 °C; (6) 120 °C; (7) 140 °C; (8) 160 °C; (9) 180 °C; and (10) 200 °C.

the impact energy of the sandwich composites manufactured, with the foam cured at the 60 °C optimized molding temperature. When the CFRP/EF sandwich composite materials were manufactured to replace the metal materials, the required optimal thicknesses could be determined and compared.

3. Results and discussion

3.1. *Properties of EF with different curing temperatures*

Fig. 2 shows the shape and some properties of EF for different curing temperatures. Fig. 2(a) shows a curve of the change of foaming volume for epoxy foams for different curing times. As the curing temperature increased, the volume of the EF initially increased with a maximum at roughly 80–90 °C after which it rather rapidly decreases rather rapidly. As shown in Fig. 2(a), at about 120 °C the color of the foam began to change implying deterioration of the foam composition at higher temperatures. Fig. 2(b) shows the cell size as a function of curing temperature along with SEM photographs of the surfaces of cured specimens with different temperatures. Fig. 3 shows schematic plots of cell and color changes EF for different curing temperatures. Based on Figs. 2 and 3, the forming shape of EF can be divided into 3 groups: 25–80 °C; 100–140 °C; and 160–200 °C. In the 25–80 °C curing group, many EF cells were formed stably and uniformly with relatively small cell size and shape and a relatively long time was required to obtain adequate curing. In the 100–140 °C curing group, unstable curing by forming reaction occurred, with increased cell size inside the form. For the 160–200 °C case a rigid layer at outside of the EF was formed much more rapidly than the foaming reaction inside the EF. A rigid layer at outside was unstably formed by high curing at curing temperatures of 160 °C or higher. The curing speed of the outside layer occurs much more rapidly than the inside foaming process. At these higher temperatures, the foaming reaction of the EF was very unstable, the cell size was large, and the EF was nonhomogeneous.

Fig. 4(a) shows the 95% curing time (determined by DSC) as a function of curing temperature. Fig. 4(b) shows specimen density and T_g as functions of the curing temperature. Since EF takes more than one day to cure at 25 °C, which is not suitable for many industrial manufacturing applications, data for this temperature is not included in the graph. The curing temperatures above 25 °C might be applicable for practical manufacturing of parts, i.e. it took about 65 and 38 min for curing temperatures of 50 and 60 °C, whereas it took less than 10 min for those above 120 °C.

Fig. 4(b) shows that as the curing temperature increases from 25 °C to 80 °C, the density of the EF initially tends to slightly decrease but then at 100 °C and above the density of the EF rather rapidly increases. T_g, on the other hand, starts out increasing rather rapidly followed by increasing at a continuously decreasing rate over the temperature range of 25 °C–200 °C. The different behaviors of the density and T_g with increasing temperature might be explained as follows. Since the epoxy resin could be cured rapidly at high temperature, while the EF was experiencing an increase in crosslink density, which could help explain the observed temperature effects on density and T_g.

Curing behavior of EF consists of three steps or phases: liquid, gel, and crosslinked. A large volume change occurs during the EF curing process which might be adjusted by lowering the curing temperature. As the EF is foamed, the curing reaction proceeded from inside to outside. The curing temperature and curing rate of the EF are interrelated. The higher the curing temperature, the more the crosslinking particularly near the surface of the EF. The speed of foaming inside the EF also increased as the curing temperature increased.

Curing temperatures from 25 to 80 °C did not significantly interfere with foaming inside the EF, although the outside of the EF quickly develops a gelation phase. As the cell size inside

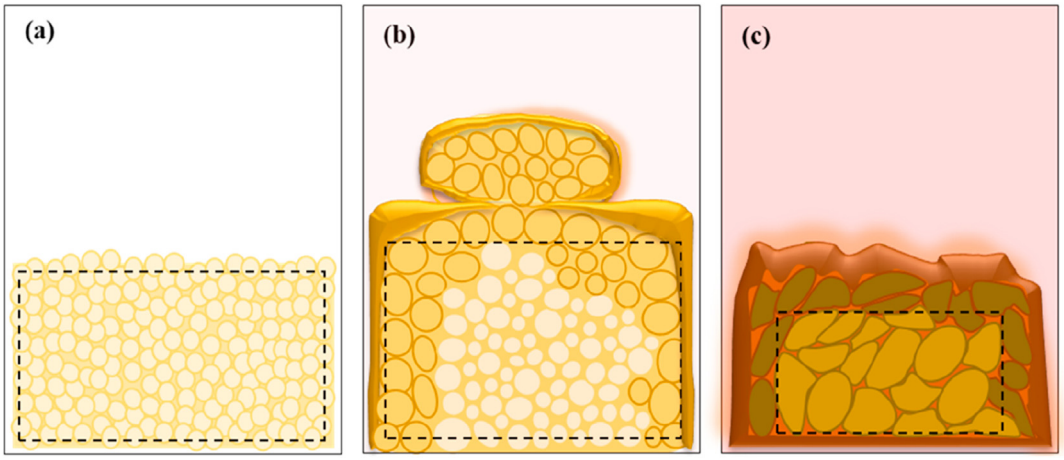

Fig. 3 – Schematic of characteristics of epoxy foams cured at different temperatures: (a) 25–80 °C; (b) 100–140 °C; and (c) 160–200 °C.

the EF increased, the density initially tended to slightly decrease. Based on the result of an increasing T_g, crosslinking of the EF also increased as the curing temperature increased. At curing temperatures of 100 °C and higher, the curing speed rapidly progresses near the outside of the foam, and the cell size inside the EF continuously increases. This may be due to the thick crosslinked layer of the skin although the foaming was unstable. The higher the curing temperature, the higher the degree of crosslinking at the EF surface. Both T_g and the density tended to increase with increasing cure temperature.

Fig. 5 shows the measured specific compressive strength of epoxy foams for different curing temperatures and times: Fig. 5(a) shows specific compressive strength of EF for the different aging temperatures while Fig. 5(b) shows the specific compressive strength as a function of time at 180 °C curing temperature. Fig. 5(a), reveals that EF formed at curing temperatures from 25 to 80 °C exhibited more optimal specific compressive strengths, which was attributed to more stably foamed EF. The specific compressive strength continuously decreased as the curing temperatures increased above 100 °C. Specimens of the EF molded at 140 °C or more exhibited fractures during compression testing. This EF crushing phenomena, the decreased specific compressive strength and cracking of specimens cured at these higher temperatures is attributed to increased cell size.

Fig. 5(b) shows the differences in specific compressive strength with aging time for EF specimens cured from 25 to 200 °C. Specific compressive strengths were clearly different for the different curing temperatures. All the EFs were aged for 180 min. The specific compressive strength of the EFs cured at 25–120 °C exhibited a relatively low reduction of about 10%, whereas the EFs cured at 140 °C or higher exhibited 20–50% decreases, ~~at~~ with 180 min aging time. As the aging time increased, the surface of the EF turned to a brown color. Even after 120 and 180 min of aging at 180 °C, the brown color depths were only 0.691 mm and 0.716 mm in the 40 mm thick foam specimens. In the case of the EF, unlike other type foams, the surface was mainly degraded by thermal aging. This aging resulted in rather small decreases in strength of the foams. As the thermal aging time increased, the color of the

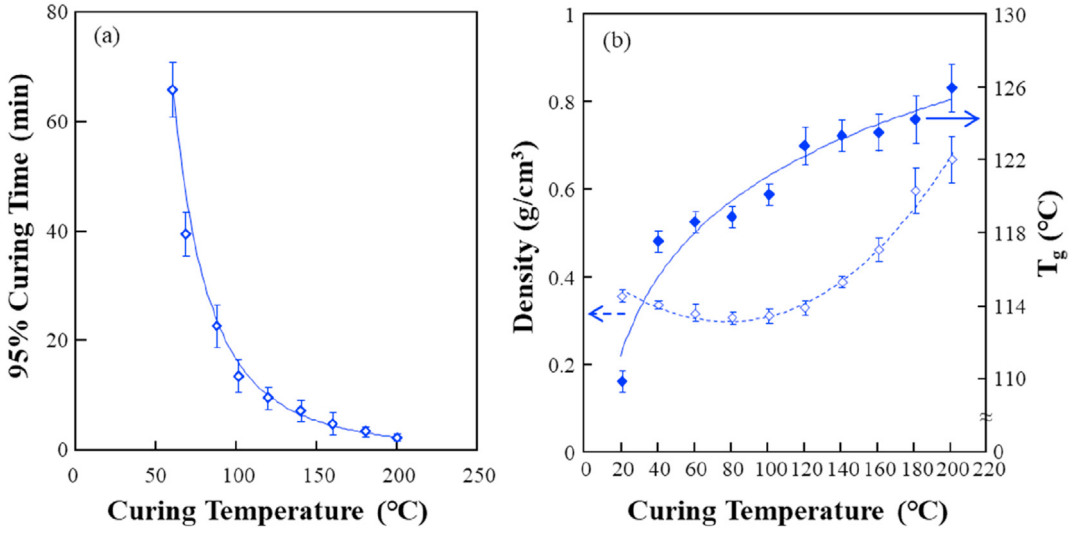

Fig. 4 – Properties of epoxy foams cured at different temperatures: (a) 95% degree of cure by DSC and (b) density and T_g.

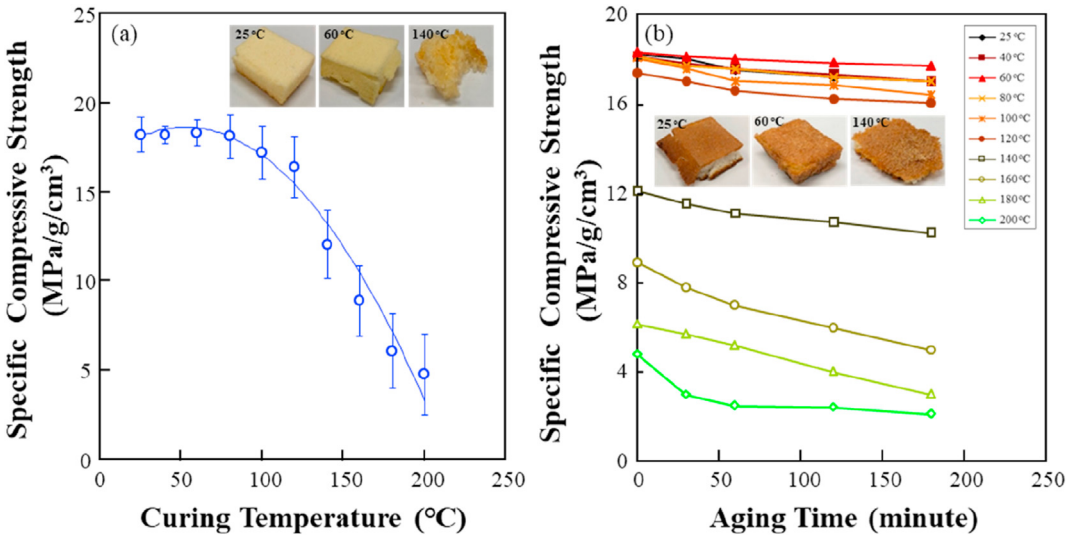

Fig. 5 – Specific compressive strength of epoxy foam (a) with different curing temperatures; and (b) with different aging temperatures.

foams changed to a darker brown and the foams experienced some fracturing under the compressive loading. For the EFs cured at 25 °C, 40 °C, and 60 °C, the color of the foams changed to a light brown and they experienced little fracturing under the compressive loading. From these results, the optimal curing temperature was roughly 60 °C which resulted in a proper curing rate, stable foam shape, low density, and high specific compressive strength.

3.2. *Mechanical properties of CFRP/EF with different curing temperatures*

Fig. 6(a) shows results of the lap shear strength (LSS) tests, used to evaluate adhesive shear strength between CFRP and EF of the sandwich composites foams with different curing temperatures. The sandwich composite specimen with EF cured at 60 °C exhibited the highest lap shear strength. Failure occurred mainly in the EF rather than at the structural adhesive interface. From this, it was concluded that proper manufacture of sandwich composites was very important to improve the strength and modulus of the EF.

Fig. 6(b) shows SEM images of the gap between cells of the EFs for different curing temperatures. The SEM images in Fig. 2(b) show that the size of the cells of the EF increased with increasing curing temperature. To prepare the LSS specimens statistically-uniformly, the EF was fabricated into specimens of identical size by trimming and entirely removing the gelation outer layer. As shown in Fig. 3, EF formed at 25 °C exhibited a relatively uniform, dense, small-sized cell spacing, whereas EF foamed at 60–80 °C had a relatively-large cell size with wide gaps between cells. However, EF foamed above 100 °C exhibited a non-uniform cell size and tight gaps between cells again, and the EF structure was easily collapsed due to thermal degradation associated with the high temperature curing. As the gap between cells increased, EF with thick epoxy layers existed a high mechanical modulus. The CFRP/EF interface was relatively stable due to mechanical interlocking effects. However, for EF foamed at a temperature of 100 °C or higher, the degree of crosslinking was high, so that the interface and foam were easily damaged by mechanical loading, resulting in low LSS results.

Fig. 7 shows a schematic model of the fracture behavior of CFRP/EF at the interface in which there are 3 different phases depending on the curing temperature. As the ageing temperature increased, the EF becomes more brittle. Both the surface roughness of the EF as well as the EF rigidity of the gap between cells influences the final mechanical performance. For the EF cured at 25 °C, since the foam itself has relatively low rigidity, the foam exhibited cohesive fracture behavior upon application of a load on the CFRP/EF. For the epoxy foam cured at 60 °C, breakage occurred near the interface between EF and the adhesive due to the increased stiffness of the EF. Improved roughness may also contribute to the enhanced interfacial adhesion. It affected that the crack was delayed between adhesive and EP foam and the more load was needed to fracture of EP foam. When the curing temperature of the EF was set at 120 °C, the interface of the EF became very brittle. When the fracture load was applied to CFRP/EF, breakage easily occurs in the brittle cells. Moreover, the surface roughness was too huge and the adhesive was not impregnated enough to epoxy foam. It affected that the load was concentrated directly to thermo-degraded epoxy foam.

Fig 8 shows plots of compressive and flexure strength of CFRP/EF sandwich composites cured at different temperatures. The curve in Fig. 8(a) shows that the maximum compressive strength of the CFRP/EF sandwich composites cured at 60 °C. Fig. 8(b) shows that the maximum flexural strength of the sandwich composites, for both the longitudinal and transverse directions, was also for specimens cured at 60 °C. The optimization of curing temperature of the EF was critical for manufacturing sandwich composites. The curing temperature conditions can cause differences in foam's properties up to 50%. Optimizing the curing temperature of the EF was to maximize the property of CFRP/EF.

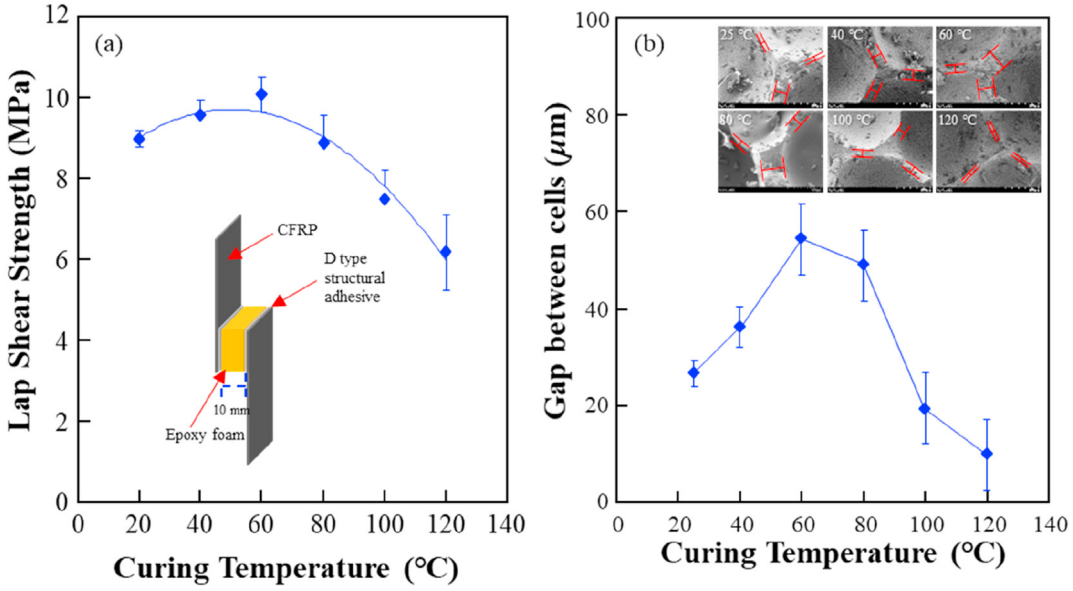

Fig. 6 – (a) Lap shear strength of the CFRP/epoxy foam sandwich composites; (b) The gap between the cells of the epoxy foams cured at different temperatures.

3.3. *Comparison of impact properties between steel and CFRP/EF sandwich composites*

Fig. 9 compares the impact properties of steel and CFRP/EF composites to verify that sandwich composites can be effectively used, as a substitute for steel in vehicle parts. The impact energies were determined using an Izod impact tester. The steels studied were those used in real vehicles. The three types of steel studied were SGARC340, SGAFC590, and SGAFC980 with three thicknesses, i.e. 0.7, 1, and 1.2 mm. The numbers at the end of the steel's name indicates it's tensile strength, i. e: steels SGARC340, SGAFC590, SGAFC980 have tensile strengths of 340.590 and 980 MPa, respectively.

The steel SGARC340, with the lowest tensile strength exhibited a large difference in the impact energy for different thicknesses i. e: for 0.7 mm thickness the impact energy was 2.5 J, whereas when the thickness increased to 1.2 mm, impact energy also increased to 9 J. In the case of the steel 590, the impact energy was 9 J at 1 mm thick and 11.5 J at 1.2 mm thick.

Overall, the higher the yield stress of the metal, the higher the impact energy and the Giga steel 980 had the highest impact strength of 14 J. In general, CFRP with a thickness of 2.4 mm has a low impact energy of less than 2 J. From the trend line, the CFRP thickness should be about 4 mm to have an impact energy equivalent to the steel 590. For a 5 mm thickness, it was expected to have an impact energy comparable to Giga steel 980. Based on the impact energy tests in this study, the thickness of CFRP should be about 5 times the thickness of the steel. The impact tests of sandwich composites fabricated with the EFs of varying thickness were conducted to determine the optimal thickness. The impact energy of composite specimens with epoxy foam approximately 7 mm thick exhibited a wide variation in impact energy ranging from 6 to 14 J. However, these composites' average impact energy was found to be close to that of steel 590 of 1 mm thickness.

EF with a thickness of 18 mm had an impact energy similar to that of Giga steel 980, and if the thickness of the epoxy foam

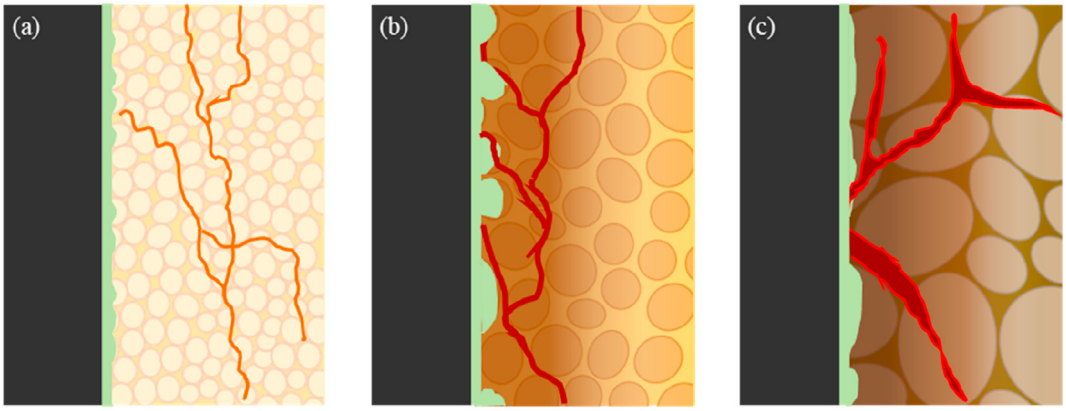

Fig. 7 – Schematic diagrams of interfacial fracture in CFRP/adhesive/epoxy foam cured at (a) 25 °C; (b) 60 °C; and (c) 120 °C.

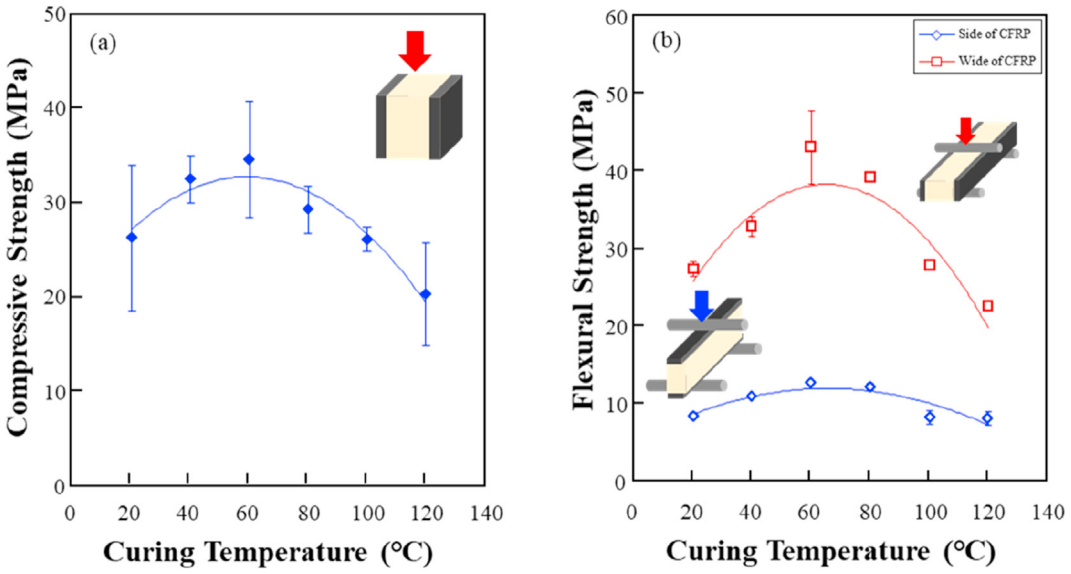

Fig. 8 – Mechanical properties of CFRP/epoxy foam sandwich composites with different curing temperatures: (a) compressive strength and (b) flexural strength.

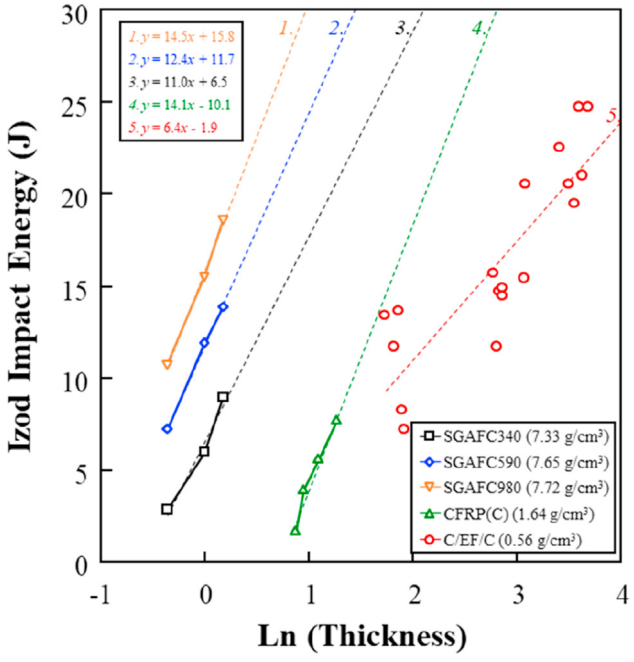

Fig. 9 – Impact energy of specimens with different conformation and thickness.

is about 35 mm, the impact energy required to replace the vehicle steels as a composite part has been achieved. Based on the results in Fig. 9, steels were not broken or fractured but only bent as much as 180° under the impact loading. However, CFRP/EF/CFRP sandwich composites showed other problem that the breakage of CFRP caused the epoxy foam to break or the carbon fiber fragments to scatter, which need to be discussed in the future following studies further.

4. Conclusions

In this study, the effects of curing temperature of epoxy foam on the formability, mechanical and thermal properties of the foam were studied. Mechanical evaluations of CFRP/EF/CFRP sandwich composites were preformed to ascertain the applicability of CFRP/EF/CFRP materials to vehicle parts. The EF exhibited increased brittleness, T_g, and cell size as the curing temperature was increased. A curing temperature of 60 °C was found to be optimal for obtaining the proper stability, compression durability, and heat stability. The mechanical properties of CFRP/EF/CFRP sandwich composites were very dependent on the curing temperature. The use of epoxy foam cured at 60 °C enhanced the adhesion in CFRP. This is attributed to the widened cell spacing, which led to strong adhesion, thus improving the compressive and flexural properties of the sandwich composites. By comparing the steel and CFRP *via* impact tests, 5 times ~~of~~ the thickness of the steel thickness was required for CFRP to have the same impact strength as the steel. Furthermore, when the impact energy of CFRP/EF/CFRP sandwich composites was compared with that of steel, sandwich composites 7 mm thick EF had the same impact energy as 1 mm thick steel 590. Composites with 18 mm thick EF, would have an impact energy equivalent to 1 mm thick Giga steel 980. These experiments and analysis demonstrate that CFRP/EF/CFRP sandwich composites may, in the future, be a promising candidate for use in vehicle parts.

Declaration of Competing Interest

The authors declare that they have no known competing financial interests or personal relationships that could have appeared to influence the work reported in this paper.

Acknowledgements

This research was supported by Basic Science Research Program through the National Research Foundation of Korea (NRF) funded by the Ministry of Education (2020R1A6A1A 03038697).

REFERENCES

[1] Fleisher J, Teti R, Lanza G, Mativenga P, Mohring HC, Caggiano A. Composite materials parts manufacturing. CIRP Ann - Manuf Technol 2018;67:603–26. https://doi.org/10.1016/j.cirp.2018.05.005.
[2] Shi H, Liu W, Fang H. Damage characteristics analysis of GFRP-Balsa sandwich beams under Fourpoint fatigue bending. Compos Part A Appl Sci Manuf 2018;109:564–77. https://doi.org/10.1016/j.compositesa.2018.04.005.
[3] Supian ABM, Sapuan SM, Zuhri MYM, Zainudin ES, Ya HH. Hybrid reinforced thermoset polymer composite in energy absorption tube application: a review. Def. Technol. 2018;14:291–305. https://doi.org/10.1016/j.dt.2018.04.004.
[4] Zhu S, Ma L, Wang B, Hu J, Zhou Z. Lattice materials composed by curved struts exhibit adjustable macroscopic stress-strain curves. Mater Today Commun 2018;14:273–81. https://doi.org/10.1016/j.mtcomm.2018.01.017.
[5] Xu C, Hu ZF, Yao C, Mo F. Experimental study on the quasi-static compression behavior of multilayer aluminum foam sandwich structure. J Alloys Compd 2019;810:151860. https://doi.org/10.1016/j.jallcom.2019.151860.
[6] Kim G, Sterkenburg R, Tsutsu W. Investigating the effects of fluid intrusion on Nomex® honeycomb sandwich structures with carbon fiber facesheets. Compos Struct 2018;206:535–49. https://doi.org/10.1016/j.compstruct.2018.08.054.
[7] Sahu S, Mondal DP, Cho JU, Goel MD, Ansari MZ. Low-velocity impact characteristics of closed cell AA2014-SiC p composite foam. Compos B Eng 2019;160:394–401. https://doi.org/10.1016/j.compositesb.2018.12.054.
[8] Zhou T, Zhang P, Xiao W, Liu J, Cheng Y. Experimental investigation on the performance of PVC foam core sandwich panels under air blast loading. Compos Struct 2019;226:111081. https://doi.org/10.1016/j.compstruct.2019.111081.
[9] Tuwair H, Drury J, Volz J. Testing and evaluation of full scale fiber-reinforced polymer bridge deck panels incorporating a polyurethane foam core. Eng Struct 2019;184:205–16. https://doi.org/10.1016/j.engstruct.2019.01.104.
[10] Sun Y, Guo LC, Wang TS, Zhong SY, Pan HZ. Bending behavior of composite sandwich structures with graded corrugated truss cores. Compos Struct 2018;185:446–54. https://doi.org/10.1016/j.compstruct.2017.11.043.
[11] Xu F, Huang DD, Du X. Improving the delamination resistance of carbon fiber/epoxy composites by brushing and abrading of the woven fabrics. Constr Build Mater 2018;158:257–63. https://doi.org/10.1016/j.conbuildmat.2017.10.015.
[12] Vemuluri RB, Rajamohan V, Sudhagar PE. Structural optimization of tapered composite sandwich plates partially treated with magnetorheological elastomers. Compos Struct 2018;208:258–76. https://doi.org/10.1016/j.compstruct.2018.05.100.
[13] Safaei B, Dastjerdi RM, Qin Z, Chu F. Frequency-dependent forced vibration analysis of nanocomposite sandwich plate under thermo-mechanical loads. Compos B Eng 2019;161:44–54. https://doi.org/10.1016/j.compositesb.2018.10.049.
[14] Liu H, Chen L, Du B, Peng S, Guo Y, Zhao Y, et al. Flatwise compression property of hierarchical thermoplastic composite square lattice. Compos Struct 2019;210:118–33. https://doi.org/10.1016/j.compstruct.2018.11.047.
[15] Zhang F, Liu W, Ling Z, Fang H, Jin D. Mechanical performance of GFRP-profiled steel sheeting composite sandwich beams in four-point bending. Compos Struct 2018;206:921–32. https://doi.org/10.1016/j.compstruct.2018.08.034.
[16] Djama K, Michel L, Gabor A, Ferrier E. Mechanical behaviour of a sandwich panel composed of hybrid skins and novel glass fibre reinforced polymer truss core. Compos Struct 2019;215:35–48. https://doi.org/10.1016/j.compstruct.2019.02.033.
[17] Sikdar S, Ostachowicz W. Nondestructive analysis of core-junction and joint-debond effects in advanced composite structure. Polym Test 2019;73:31–8. https://doi.org/10.1016/j.polymertesting.2018.11.011.
[18] Hazrati A. Multi-scale analysis of nonlinear fatigue damage behaviour of a quad-core sandwich panel with heterogeneous aluminium sheets. Theor Appl Fract Mech 2019;99:79–94. https://doi.org/10.1016/j.tafmec.2018.11.003.
[19] Ha GX, Zehn MW. Experimental study and finite element simulation of novel nap-core sandwich composite. Compos B Eng 2019;158:117–30. https://doi.org/10.1016/j.compositesb.2018.09.053.
[20] Seguel F, Meruane V. Damage assessment in a sandwich panel based on full-field vibration measurements. J Sound Vib 2018;417:1–18. https://doi.org/10.1016/j.jsv.2017.11.048.
[21] Wang C, Murugadoss V, Kong J, He Z, Mai X, Shao Q, et al. Overview of carbon nanostructures and nanocomposites for electromagnetic wave shielding. Carbon 2018;140:696–733. https://doi.org/10.1016/j.carbon.2018.09.006.
[22] Shu C, Zhao S, Hou S. Crashworthiness analysis of two-layered corrugated sandwich panels under crushing loading. Thin-Walled Struct 2018;133:42–51. https://doi.org/10.1016/j.tws.2018.09.008.
[23] Smorygo O, Gokhale AA, Vazhnova A, Stefan A. Ultra-low density epoxy/polystyrene foam composite with high specific strength and pseudo-plastic behavior. Compos Commun 2019;15:64–7. https://doi.org/10.1016/j.coco.2019.06.008.
[24] Khundamri N, Aouf C, Fulcrand H, Dubreucq E, Tanrattanakul V. Bio-based flexible epoxy foam synthesized from epoxidized soybean oil and epoxidized mangosteen tannin. Ind Crop Prod 2019;128:556–65. https://doi.org/10.1016/j.indcrop.2018.11.062.
[25] Wang L, He Y, Jiang T, Zhang X, Zhang C, Peng X. Morphologies and properties of epoxy/multi-walled carbon nanotube nanocomposite foams prepared through the free-foaming and limitedfoaming process. Compos Sci Technol 2019;182:107776. https://doi.org/10.1016/j.compscitech.2019.107776.
[26] Sahu SK, Badgayan ND, Samanta S, Sahu D, R Sreekanth PS. Influence character of cell size on out of plane stiffness and in-plane compliance of the sandwich beam made with tunable PCTPE nylon honeycomb core and hybrid polymer nanocomposite skin. Int J Mech Sci 2018;148:284–92. https://doi.org/10.1016/j.ijmecsci.2018.08.011.
[27] Choi JY, Kwon IJ, Park SM, Kwon DJ. Investigation of properties of structural foam with different conformation and via thermal aging condition. Compos Res 2018;31(4):122–7. https://doi.org/10.7234/composres.2018.31.4.122.
[28] Kwon DJ, Kim JH, Park SM, Kwon IJ, Park JM. Investigation of compressive strength and foaming characteristics of acid

anhydride epoxy foam by foaming agent. Compos Res 2018;31(4):133–8. https://doi.org/10.7234/composres.2018.31.4.133.

[29] Zhang X, Li B, Wang X, Li K, Wang G, Chen J, et al. Modification of iPP microcellular foaming behavior by thermal history control and nucleating agent at compressed CO_2. J Supercrit Fluids 2018;133:383–92. https://doi.org/10.1016/j.supflu.2017.11.003.

[30] Alonso MV, Auad ML, Nutt SR. Modeling the compressive properties of glass fiber reinforced epoxy foam using the analysis of variance approach. Compos Sci Technol 2006;66:2126–34. https://doi.org/10.1016/j.compscitech.2005.12.016.

[31] Li TT, Dai W, Huang SY, Lou CW, Lin JH. Preparation and characterization of SEBS-g-MAH-filled flexible polyurethane foam composites with gradient-changing structure. Mater Des 2019;183:108150. https://doi.org/10.1016/j.matdes.2019.108150.